Blockade by NNC 55-0396, mibefradil, and nickel of calcium and exocytotic signals in chromaffin cells: implications for the regulation of hypoxia-induced secretion at early life

*José C. Fernández-Morales[1,2], *J. Fernando Padín[1,2], Stefan Vestring[1,4], Diego C. Musial[1,2,5], Antonio-Miguel G. de Diego[1,2] and Antonio G. García[1,2,3]

[1]Instituto Teófilo Hernando; [2]Departamento de Farmacología y Terapéutica, Facultad de Medicina, Universidad Autónoma de Madrid, Spain. [3]Servicio de Farmacología Clínica, Instituto de Investigación Sanitaria, Hospital Universitario de la Princesa, Madrid, Spain. [4]Medizinische Fakultät Carl Gustav Carus, Technische Universität Dresden,Germany. [5]Department of Pharmacology, Federal University of São Paulo (UNIFESP), São Paulo, SP, Brazil.

Contact information:

Antonio G. García
Instituto Teófilo Hernando
Departamento de Farmacología, Facultad de Medicina
Universidad Autónoma de Madrid
Avda. Arzobispo Morcillo, 4
28029, Madrid (Spain)
Phone number: +34914973120/21
Fax number: +34914975380

e-mail: agg@uam.es

*Equal contributors

Quantitative data:

Number of pages: 27

Number of figures: 7

Number of tables: 1

Number of references: 39

Abstract: 182 words

Introduction: 711 words

Discussion: 1169 words

Abreviations:

Chromaffin cells (CCs); voltage activated calcium channels (VACCs); bovine chromaffin cells (BCCs); rat embryo chromaffin cells (RECCs); cytosolic Ca^{2+} concentrations ($[Ca^{2+}]_c$); hypoxia-induced secretion (HIS).

Summary

Adrenal chromaffin cells (CCs) express high-voltage activated calcium channels (VACCs) of the L, N and PQ subtypes; additionally, T-type low-VACCs are also expressed during embryo and neonatal life. Effects of the more frequently used T channel blockers NNC 55-0396 (NNC), mibefradil, and Ni^{2+} on the whole-cell Ba^{2+} current (I_{Ba}), the K^+-elicited $[Ca^{2+}]_c$ transients and catecholamine secretion, have been studied in adult bovine CCs (BCCs) and rat embryo CCs (RECCs). NNC, mibefradil, and Ni^{2+} blocked BCC I_{Ba} with IC_{50} of 1.8, 4.9 and 70 μM, while IC_{50} to block I_{Ba} in RECCs were 2.1, 4.4 and 41 μM. Pronounced blockade of K^+-elicited $[Ca^{2+}]_c$ transients and secretion was also elicited by the three agents. However, the hypoxia-induced secretion (HIS) of catecholamine in RECCs was blocked substantially (75%) with thresholds concentrations of NCC (IC_{20} to block I_{Ba}); this was not the case for mibefradil and Ni^{2+} that required higher concentrations to block the HIS response. Thus, out of the three compounds, NNC seemed to be an adequate pharmacological tool to discern the contribution of T channels to the HIS response, without a contamination with high-VACCs blockade.

Keywords: bovine chromaffin cells, hypoxia, calcium, NNC 55-0396, rat embryo chromaffin cells, voltage activated calcium channels.

1. **INTRODUCTION**

Up to ten members of the voltage-activated calcium channel family (VACCs) serving distinct roles in cell signaling, have been identified in mammals (Catterall, 1998). High-VACCs are targeted by several selective toxins and organics compounds; thus, N-type channels (α_{1B}, Cav2.2) is blocked by ω-conotoxin MVIIA, PQ-type (α_{1A}, Cav2.1) is blocked by ω-conotoxins MVIIC and MVIID, L-type (α_{1S}/Cav1.1, α_{1C}/Cav1.2, α_{1D}/Cav1.3, α_{1F}/Cav1.4) is targeted by 1,4-dihydropyridines derivatives blockers (nifedipine) and activators (Bayk8644), and R-type (α_{1E}/Cav2.3) is blocked by SNX-482 (de Diego et al., 2014). In contrast, the blockers of T-type low-VACCs (α_{1G}/Cav3.1, α_{1H}/Cav3.2, α_{1I}/Cav3.3) so far available have poorer selectivity. For instance nickel (Ni^{2+}) is more selective than cadmium (Cd^{2+}) (Carbone & Lux, 1984). However, this selectivity is true for α_{1H} channels but not for α_{1G} and α_{1I} that are blocked by Ni^{2+} only at concentrations that also block high-VACCs (Lee et al., 1999). Mibefradil was initially developed as a selective T channel blocker (Mishra & Hermsmeyer, 1994; Randall & Tsien, 1997; Todorovic & Lingle, 1998). However, mibefradil also blocks high-VACCs (Fang & Osterrieder, 1991; Bezprozvanny & Tsien, 1995; Viana et al., 1997). Later on, mibefradil derivative NNC 55-0396 (NNC) emerged as a more selective T-type channel blocker (Huang et al., 2004; Li et al., 2005). Unfortunately, a selective T channel blocker with potential scare side effects is still an unmet therapeutic goal (Arranz-Tagarro et al., 2014).

In adrenal medullary chromaffin cells (CCs), the use of selective blockers of high-VACCs has revealed their relative density and their contribution to the regulation of Ca^{2+} signalling and the exocytotic release of catecholamine (García et al., 2006; Mahapatra et al., 2012). Thus, in bovine chromaffin cells (BCCs) the whole cell Ca^{2+} or Ba^{2+} currents (I_{Ca}, I_{Ba}) are carried 20% by L channels, 35% by N channels, and 45% by PQ channels. Furthermore, in adult rat CCs I_{Ca} is carried 50% by L channels, 30% by N channels, and 20% by PQ channels (Gandía et al., 1995). On the other hand, in rat embryo CCs (RECCs) I_{Ca} is carried 60% by L channels and 40% by non-L channels (N/PQ) (Fernández-Morales et al., 2014). While in BCCs PQ channels dominate

the control of exocytosis, in adult rat CCs secretion is mostly controlled by L-channels (Fernández-Morales et al., 2009).

Although RECCs also express T channels, one study concluded that they played no role in controlling the depolarisation-evoked exocytosis (Bournaud et al., 2001); in contrast a more recent study suggested that the control of hypoxia-induced secretion (HIS response) was exerted by T channels (Levitsky & López-Barneo, 2009). However, in another four studies it was concluded that the HIS response in RECCs or neonate CCs was mostly controlled by L channels (Adams et al., 1996; Thompson et al., 1997; Takeuchi et al., 2001; Fernández-Morales et al., 2014).

We planned the present investigation to add some further insight in the question of the contribution of T channels to the HIS response of chromaffin cells at early life. We made a pharmacological approach to the problem by using NNC, mibefradil, and Ni^{2+} (Carbone et al., 2014). Because of their known limited selectivity discussed above, we first performed full concentration-response curves to define comparatively their IC_{20}, and IC_{50} to block the whole-cell inward Ba^{2+} current (I_{Ba}) through the high-VACCs of adult BCCs and REECs. Then we explored their effects on the K^+-elicited $[Ca^{2+}]_c$ transients and secretion in both cell types. Finally, we choose the IC_{20} concentration of the three compounds that caused little inhibition of I_{Ba} and tested its effects on the HIS response in RECCs. We found that although the three compounds fully blocked I_{Ba} in a concentration- and time-dependent manner, the threshold concentration of the tree compounds partially blocked the HIS response, NNC being the compound inducing the maximal blockade. This adds further evidence in support of T channels playing a role in the control of such response at early life. How to explain the full blockade of the HIS response by L channel blockade and at the same time, its pronounced blockade by T channel blockade, and the interaction of L an T channels in the regulation of such response, are interesting questions that require new experimental approaches. The use of low concentrations

of nifedipine and NNC with cell exposure sufficient to reach drug-receptor equilibrium may help to answer those questions.

2. MATERIAL AND METHODS

All experimental procedures with animals have been carried out following the guideline approved by the Ethical Committee for the care and use of animals of the Medical School, Autonomous University of Madrid, Spain, in accordance with the European Community Council Directive 2010/63/EEC and with the Spanish Real Decreto RD 53/2013. All efforts were made to minimise animal suffering.

2.1. Culture of bovine and rat embryo adrenal medulla chromaffin cells

BCCs were isolated from adrenal glands of calves (*Bos Taurus*), according to standard methods with some modifications (Moro et al. 1990). After digestion of the adrenal medulla with collagenase, purification of BCCs was achieved by several consecutive centrifugations. Cells were suspended in Dulbecco's modified Eagle's medium (DMEM) supplemented with 5% fetal bovine serum, 50 IU/mL penicillin, and 50 µg/mL streptomycin. For preventing the excessive growth of fibroblasts, proliferation inhibitors (10 µM cytosine arabinoside, 10 µM fluorodeoxyuridine, and 10 µM leucine methyl ester) were added to the medium.

Rats were housed individually under controlled temperature and lighting conditions with food and water provided *ad libitum*. Chromaffin cells were obtained from 18-day-old (E18) rat embryos by a protocol previously described for mice (Sorensen et al., 2003) with some modifications. The pregnant Wistar rat was killed by decapitation; the fetuses were rapidly extracted and immediately decapitated. Adrenal glands were then rapidly removed from the embryos, fat-trimmed, and introduced in 1 ml of an enzymatic solution containing 20 U/ml of papain. Adrenals were digested for 20 min; 1 ml of another solution (10% fetal bovine serum, 2.5 mg/ml albumin from bovine serum and 2.5 mg/ml trypsin inhibitors) to stop the enzymatic reaction was then added for 15 s. The cell suspension was centrifuged for 4 min at 104 g, the

supernatant was removed, and the cell pellet was gently resuspended with 0.8 to 1.5 ml of DMEM, depending on the final desired cell density. A 100- to 120-µl drop of cell-containing solution was plated on poly-D-lysine-coated coverslips of one 12-well plates (for secretion experiments) or on 6-well plates (for patch-clamp and $[Ca^{2+}]_c$ transients experiments). After 1 h in an incubator, DMEM (1 ml for 12-well plates and 2 ml for 6-well plates) supplemented with 4% fetal bovine serum, 50 IU/ml penicillin and 50 µg/ml streptomycin was added to each well. Experiments were done in cells that were kept in a water-saturated incubator at 37 °C and a 5% CO_2 atmosphere for 1 to 2 days.

2.2. Recording of whole-cell barium currents

For patch-clamp recording of I_{Ba} the perforated-patch mode of the patch-clamp technique was used, with amphotericin B as the permeating agent. Tight seals (>5 GΩ) were achieved in a bath solution for recording I_{Ba} (standard Tyrode solution) composed of the following (in mM): 137 NaCl, 1 $MgCl_2$, 5 $BaCl_2$, 5.3 KCl, 10 glucose, and 10 HEPES and 0.001 tetrodotoxin, pH 7.3 adjusted with NaOH. The intracellular solution for the recording of I_{Ba} under voltage-clamp conditions contained (in mM): 145 glutamic acid, 1 $MgCl_2$, 8 NaCl and 10 HEPES, pH 7.2 with CsOH. I_{Ba} was recorded at room temperature (22 ± 2 °C) by means of an EPC-10 patch-clamp amplifier (HEKA Elektronik, Lambrecht, Germany) controlled by PULSE software running on a personal computer. The access resistance was monitored until it decreased to < 20 MΩ. *R*s averaged 8.6 ± 0.3 MΩ in BCCs and was always compensated by 95%. In all recordings the holding potential was –80 mV. I_{Ba} was activated in response to 50-ms depolarising 10 mV voltage steps from –60 to +60 mV. The test voltage protocol was applied every 15 s. Current signals were filtered at 5 kHz, digitised at 50 kHz, and on-line leak subtracted via a P/4 protocol.

2.3. Measurements of changes of the cytosolic calcium concentrations

To monitor the changes of $[Ca^{2+}]_c$, chromaffin cells were incubated for 1 h at 37º C in DMEM containing the Ca^{2+} probe Fura-2 AM (10 μM). After this incubation period, the coverslips were mounted in a chamber and cells were washed and covered with Tyrode solution composed of (mM) 137 NaCl, 1 $MgCl_2$, 5.3 KCl, 2 $CaCl_2$, 10 HEPES, and 10 glucose, pH 7.3 with NaOH. The setup for fluorescence recordings was composed of a Leica DMI 4000 B inverted light microscope (Leica Microsystems; Barcelona, Spain) equipped with an oil immersion objective (Leica 40x Plan Apo; numerical aperture 1.25). The cells were continuously superfused by means of a five-way superfusion system at 1 ml/min with a common outlet 0.28 mm-tube driven by electrically controlled valves with Tyrode's solution. Fura-2 was excited alternatively at 340 ± 10 and 387 ± 10 nm using a Küber CODIX xenon 8 lamp (Leica). Emitted fluorescence was collected through a 540 ± 20 nm emission filter and measured with an intensified charge coupled device camera (Hamamatsu camera controller C10600 orca R2; Japan). Fluorescence images were generated at 1-s intervals. Images were digitally stored and analysed using LAS AF software (Leica; Barcelona, Spain). A Tyrode external solution of the same composition as the one described above was used; drugs were dissolved in this solution.

2.4. Amperometric recordings of single-vesicle quantal catecholamine release

Amperometry was chosen to measure catecholamine release at the single cell level. Electrodes were built as previously described (Wightman et al. 1991). The amperometer was homemade (Universidad Autónoma de Madrid workshop) and was connected to an EPC-10 patch-clamp amplifier (HEKA, Lambrecht, Germany) that digitised the signal at 10 kHz sending it to a Microsoft personal computer (PC). A 700 mV potential was applied to the electrode with respect to an AgCl ground electrode. The electrodes were calibrated according to good amperometric practices by perifusing 50 μM noradrenaline dissolved in standard Tyrode's solution and measuring the current elicited; only electrodes that yielded a current between 200 and 400 pA were used. The coverslips were mounted in a chamber on a Nikon Diaphot inverted microscope (Nikon, Tokyo, Japan) used to localize the target cell, which was continuously

superfused by means of an eight-way superfusion system with a common outlet driven by electrically controlled valves, with a Tyrode solution composed of (in mM): 137 NaCl, 1 $MgCl_2$, 5.3 KCl, 2 $CaCl_2$, 10 HEPES, and 10 glucose, pH 7.3 with NaOH. The high K^+ solutions were prepared by replacing equiosmolar concentrations of NaCl with KCl. At the time of experiment performance, proper amounts of drug stock solutions were freshly dissolved into the Tyrode solution and the high-K^+ solutions.

2.5. Data analysis and statistics

The analysis of I_{Ba} amplitude was measured at the maximum peak current obtained with a 50-ms test pulse to 0 mV. Only the cells that held up the entire protocol (control, blocker and wash) were included in the statistics. We used a Student´s t test for paired comparisons between normalised values between I_{Ba} peak before and during blocker treatment. Data are expressed as means ± S.E.M. of the number of cells and cultures indicated in parentheses.

Regarding the changes of $[Ca^{2+}]_c$, the data analysis was carried out on a PC; data obtained from LAS AF software or Ascent software version 2.4.2, were exported to Excel tables (Microsoft, Redmond, WA). Graphs and the mathematical analyses were performed using the Graphpad Prism software, version 5.01 (GraphPad Software Inc., San Diego, USA). Peak heights were calculated by integrating the $[Ca^{2+}]_c$ transient over time during the stimulus duration by means of Origin Pro 8 SR2 software, version 8.0891 (OriginLab Corporation, Northampton, USA).

For amperometric recordings, data analysis was carried out on a PC using Excel (Microsoft, Redmond, WA) and IgorPro (Wavemetrics, Lake Oswego OR). Amperometric charge (Q_{amp}) was calculated by integrating the amperometric current over time during the stimulus duration with a macro written in IgorPro. The number of spikes greater than 7 pA was manually counted on an extended graph displayed in the computer screen. A ruler was drawn at 7 pA, and spikes going above the threshold amplitude were considered. Differences between means of group data fitting a normal distribution were assessed by using either analysis of variance or Kruskal-

Wallis test for comparison among multiple groups, or Student's t test for comparison between two groups. $P < 0.05$ was taken as the limit of significance. Only the cells that responded with more than 20 spike events during an initial 10-s period of the high K^+ pulse and that held up the entire protocol (control, drug exposure and wash) were included in the statistics. Data are represented as mean ± S.E.M. obtained in cells from at least 3 different cultures. *P<0.05; **P<0.01 with respect to control, Mann-Whitney's rank-sum test; $P < 0.05$ was taken as the limit of significance.

2.6. *Chemical products*

Products to make saline solutions, NNC 55-0396 (PubChem CID: 11957578), mibefradil (PubChem CID: 16219666), and $NiCl_2$ were purchased from Sigma-Aldrich, Madrid, Spain. The following chemicals were used for cell culture: DMEM (Dulbecco's Modified Eagles Medium) and penicillin-streptomycin were from GIBCO, Scotland, UK, fetal bovine serum was from PAA laboratories, Pasching, Austria, and papain was from Worthington, Lakewood, NJ. The probe Fura-2AM was supplied by Invitrogen, Eugene, Oregon, USA.

3. RESULTS

In this investigation three parameters were monitored namely, I_{Ba}, $[Ca^{2+}]_c$ transients, and secretion of catecholamine. These three responses are triggered by cell depolarisation that causes Ca^{2+} entry through VACCs, an elevation of the $[Ca^{2+}]_c$, and the Ca^{2+}-dependent release of catecholamine (García et al. 2006). The effects of NNC, mibefradil, and Ni^{2+} on these three parameters were tested in parallel in BCCs and RECCs. Additionally, we also studied the HIS response in RECCs and the effects of threshold concentrations of the three compounds on such response.

3.1. Calcium channel currents

The whole-cell inward VACCs currents were monitored in cells voltage-clamped at -80 mV under the perforated-patch mode of the patch-clamp technique, using 5 mM Ba^{2+} as charge

carrier (I_{Ba}). Ba^{2+} was used because the current was small when using Ca^{2+} as charge carrier in RECCs. Test depolarising pulses of 50 ms duration were sequentially applied at 15-s intervals. Under these conditions the effects of NNC could be tested in the same cell in a sandwich-type experiment: the initial test pulses generated control currents, then the compound was added and finally, it was withdrawn from the superfusion medium to check whether the blocking effect was reversible. With NNC the reversibility was slow and partial; thus, a single concentration of the compound was tested in every cell. Experiments in BCCs and RECCs were done in parallel. The mean I_{Ba} amplitude in 137 BCCs was 440± 0.321 pA (± S.EM.); in 122 RECCs I_{Ba} amplitude was 253 ± 12 pA. These values are consistent with a higher surface of BCCs (9.87± 0.31 pF; n=115 cells) with respect RECCs (6.27± 0.17 pF; n=82 cells).

Fig. 1 summarises the pattern of I_{Ba} blockade elicited by single or increasing concentrations of NNC. Panel A shows a family of I_{Ba} traces generated by depolarising test pulses given at 10 mV steps from -60 to +60 mV, applied on an example BCC (A,a). As expected from the use of Ba^{2+} as charge carrier, I_{Ba} did not inactivate. In the presence of 5 μM NNC, the current traces were blocked by 70% (A,b). After 5 min of NNC washout, the currents recovered only partially (A,c). I-V curves before (control), during NNC perifused at 1 μM (NNC), and after NNC washout are graphed in panel B. Threshold current was at -30 mV, peak current at 0 mV, and the reversal potential at +60 mV. At 1 μM, NNC blocked I_{Ba} by 40% but there was no shift of the I-V curve; at this low concentration, the peak current recovered its control value after 5 min of NNC removal. Panel C shows a concentration-response curve for the blocking effects of NNC on I_{Ba}. The threshold concentration was at 30 nM, the IC_{50} was 1.86 μM, and full blockade was achieved at 10 μM.

Fig. 1D,E,F summarises the results obtained with NNC in REECs. The family of control I_{Ba} currents (Da) are reduced by 70% in the presence of 5 μM NNC (Db), with an incomplete recovery after 5 min of compound washout (Dc). In the I-V curves of panel E, the threshold I_{Ba} was at -50 mV, the peak current at -10 mV, and the reversal potential at -60 mV; in the presence

of 1 μM NNC, I_{Ba} peak was reduced by 35% with full recovery upon compound washout. The concentration-response curve of panel F shows a threshold concentration at around 50 nM, an IC_{50} of 2.09 μM, and 75% of current blockade at 10 μM. The blockade elicited by mibefradil exhibited characteristics similar to those of NNC. Of interest was the fact that at 5 μM mibefradil shifted to the left the I-V curve for I_{Ba} by 10 mV (not shown) in RECCs but not in BCCs. Fig. 2A shows that in BCCs the threshold blockade is between 30 and 100 nM, the IC_{50} is at 4.95 μM, and full current blockade was achieved at 30 μM. Similar outcomes were found in RECCs, with an IC_{50} of 4.45 μM. In BCCs Ni^{2+} exerted a concentration-dependent blockade of I_{Ba}, with threshold concentrations at around 5 μM, IC_{50} of 70 μM and full blockade at 1 mM (Fig. 2C). In RECCs a somehow lower IC_{50} was obtained namely, 41 μM; threshold and full blockade concentrations were similar to those of BCCs, around 5 μM and 1 mM (Fig. 2D).

3.2. Time course of the induction of I_{Ba} blockade and of its reversibility

To study the time course of the induction of I_{Ba} blockade elicited by NNC, and the degree of recovery of the initial current amplitude upon withdrawal of the compound from the perifusing external solution, CCs were voltage-clamped at -80 mV and continuously challenged with test depolarising pulses to 0 mV applied with a cadence of 15 s. Because NNC caused full blockade of I_{Ba} at 50 μM (Fig. 1C) it was expected that this high concentration of the compound would cause full blockade of the current in few seconds. This was not the case, as illustrated in the example BCC of Fig. 3A. During the first minute of cell exposure to NNC, a tiny blockade of I_{Ba} was initiated. Such blockade developed faster after 1 min but took near 2 additional minutes to reach the full current blockade. After 3 min exposure to NNC, its removal gave rise to the initiation of an extremely slow recovery phase; in fact after 5 min, the I_{Ba} amplitude was only 12% of the initial (Fig. 3A). In the RECC shown in Fig. 3B, the outcome was similar to the BCC namely, an initial phase of slow and gradual blockade that lasted 2 min and then a faster phase that reached full blockade in 2 min. Again, the rate of I_{Ba} recovery after NNC washout was less than 10% in 5 min.

The initial phase of slow blockade induced by NNC was absent in the BCC displayed in Fig. 3C and exposed to 50 μM mibefradil. The blockade was initiated from the very beginning of cell exposure to the compound and took about 2.5 min to reach full current blockade. As for NNC, the washout of mibefradil after exposure to this high concentration was very slow; after 6 min of washout only about 15% of the initial I_{Ba} was recovered. The blockade and recovery were clearly concentration-dependent. For instance, the RECC of Fig. 3D was perifused with 10 μM mibefradil that gave rise to a gradual blockade that did not reach equilibrium because the compound was removed after only 2 min of cell exposure. At this lower concentration, the rate of current recovery was faster although curiously, it reached a plateau after a minute or so at about 50% of the fraction of current initially blocked. For the sake of comparison, the time course of the blockade instauration and the exit from blockade, was studied with inorganic nickel. At 50 μM, Ni^{2+} produced a fast decrease of I_{Ba} in about 15 s in both the BCC (40% blockade, Fig. 3E) and the ECC explored (60% blockade, Fig. 3F). The recovery was also rapidly (15 s) and fully established after the removal of Ni^{2+} from the external solution.

3.3. Elevations of the cytosolic Ca^{2+} concentrations triggered by K^+ depolarisation

Blockade of VACCs by NNC should be paralleled by a similar blockade of the K^+-induced $[Ca^{2+}]_c$ transients. This happened to be the case as exemplified in the fura-2-loaded BCC and RECC that responded to successive K^+ pulses (45 mM K^+, 5 s) given at 3 min intervals, with initial transient elevations of $[Ca^{2+}]_c$ (Fig. 4A, C). At 10 μM, NNC drastically reduced the $[Ca^{2+}]_c$ transient amplitude in a clear time-dependent manner in the BCC of Fig. 4A. Upon NNC withdrawal, a partial time-dependent recovery was produced. The blockade exerted by NNC on the RECC was more gradual and scarcely reverted upon NNC washout (Fig. 4C). The concentration-response curves clearly indicated the time-dependence of the induction of the blockade elicited by NNC in both BCCs (Fig. 4B) and RECCs (Fig. 4D). It was somehow puzzling that in RECCs NNC could not fully block the $[Ca^{2+}]_c$ transients, even after 7 min

exposure to the higher concentrations used (Fig. 4D). In BCCs, however, about 90% blockade was achieved after 7 min exposure to NNC (Fig. 4B).

The effects of mibefradil on BCCs were superimposable to those of NNC; the compound effects exhibited a time-dependence with 40% blockade after 1 min exposure and over 80% blockade at the 7th minute (Fig. 5A). The blockade was also time dependent in RECCs, 40% after 1 min and 75% after 7 min (Fig. 5B). It was somehow surprising that the blocking effects of Ni^{2+} also exhibited some time dependence in BCCs, particularly at the concentrations of 10-30 μM (Fig. 5C). In RECCs the time dependence of the blockade was less pronounced but the maximum blockade achieved was about 50-60% (Fig. 5D).

3.4. Quantal catecholamine release responses triggered by high K^+

To study the effects of NNC, mibefradil, and Ni^{2+} on the quantal release of catecholamine, single BCCs or RECCs were stimulated 3-4 times with pulses of a high K^+ solution (75 mM K^+, 30 s). The spike amperometric responses of example BCC and RECC are shown in Fig. 6A, B. An initial spike burst was usually followed by more infrequent spikes along the K^+ stimulation period. This protocol produces quite reproducible responses within the same cell (not shown). At 5 μM, NNC elicited near full blockade of the response in the BCC and the RECC; partial time-dependent recovery was observed in both cell types after NNC washout (Fig. 6A, B). Pooled data showed that in BCCs, 5 μM NNC blocked by over 80% the spike number and total secretion (Qamp), with partial recovery at 5-10 min after washout (Fig. 6C). Mibefradil at 5 μM also caused 90% blockade with time-dependent full recovery of the response after washout (Fig. 6D). At 50 μM, Ni^{2+} caused near full blockade of secretion with partial recovery at 5 min after washout (Fig. 6E). The blockade elicited by NNC and mibefradil in RECCs was around 80% (Fig. 6F, G) but 50 μM Ni^{2+} caused only around 65% blockade (Fig. 6H).

3.5. Effects of threshold concentrations of NNC, mibefradil, and Ni^{2+} on the hypoxia-induced secretion in rat embryo chromaffin cells.

We have defined the threshold concentrations of NNC, mibefradil, and Ni^{2+} as those concentrations that achieve 20% blockade of the high-VACCs current (Fig. 1 and 2) namely, 0.4 μM NNC, 0.9 μM mibefradil, and 25 μM Ni^{2+}. The HIS response seems to be mediated by high-VACCs as well as low-VACCs (see Discussion). Because of the apparent selectivity of these three compounds on T-type currents (see Introduction) it was reasonable to test whether the threshold concentrations to block the high-VACCs could elicit a blockade of the HIS response more pronounced than that expected from only 20% blockade of I_{Ba}.

Cells were exposed 3 times to a 1 min hypoxia (less than 5% O_2), that produced secretory spike events along the time period of hypoxia; those responses were quite similar at hypoxia pulses P1 and P2 (Fig. 7A, B) and decreased by 16±8% for Qamp and 17 ± 8% for spike number during P3 (Fig. 7B; n=18 control cells). Given 5 min before and during the hypoxia exposure, 0.4 μM NNC caused as much as 73 ± 5% blockade of Qamp and 76 ± 1.7 blockade of spike number; recovery was complete after 5 min washout (Fig. 7C). At 0.9 μM, mibefradil inhibited the HIS response by 35 ± 6.7% (Qamp) and 37 ± 6.2% (spike number); recovery after 5 min washout was near 80% (Fig. 7D). Finally, 25 μM Ni^{2+}caused around 50% blockade of the HIS response with full recovery after washout (Fig. 7E).

4. DISCUSSION

In line with the general belief that reputed blockers of the T-subtype of low-VACCs also target the high-VACCs (García et al., 2006; Catterall, 2012; Mahapatra et al., 2012; Carbone et al., 2014), we have found here that NNC, mibefradil and Ni^{2+} caused a full concentration-dependent blockade of CC I_{Ba} and hence, of the three subtypes of high-VACCs expressed by BCCs and RECCs namely, L, N, and PQ. Of interest was the observation that the three compounds exhibited similar potencies to block I_{Ba} in RECCs and BCCs (see their IC_{20} and IC_{50} in table 1). A natural consequence of I_{Ba} inhibition was the mitigation of the K^+-elicited $[Ca^{2+}]_c$ transients that are initially shaped by the Ca^{2+} entering through the VACCs, opened by membrane depolarisation (Douglas & Poisner, 1961). However, the incomplete blockade of the K^+-elicited

$[Ca^{2+}]_c$ transients exerted by NNC, mibefradil, and Ni^{2+} contrasts with the full blockade of I_{Ba} . These differences could be explained on the basis of the different protocols used to monitor I_{Ba} (50 ms depolarising pulses) and the $[Ca^{2+}]_c$ changes (5 s of K^+ depolarisation). While in the first case the Ca^{2+} entering the cell through VACCs is the only variable implicated, in the second case the $[Ca^{2+}]_c$ transient is shaped by Ca^{2+} entry but also by its redistribution and clearance by the endoplasmic reticulum (Alonso et al., 1999) and mitochondria (Montero et al., 2000). Furthermore, the inactivation of VACCs does not occur when measuring I_{Ba} (Hernández-Guijo et al., 2001), but it is important with K^+ depolarisation produced during several seconds (Villarroya et al., 1999).

An additional feature of the blockade of I_{Ba} and the $[Ca^{2+}]_c$ transients was its time dependence; in the case of Ni^{2+} the blockade developed in few seconds, but lasted a few minutes to reach equilibrium in the case of NNC and mibefradil. Also the recovery from blockade of the two parameters was slow for NNC and mibefradil; in fact, in the case of NNC the recovery was meager after 10 min washout. This behaviour reminds the slow time course of I_{Ba} blockade and its slow recovery in BCCs exerted by lipophilic compounds such as R56865 (Garcez-do-Carmo et al., 1993), dotarizine and flunarizine (Villarroya et al., 1995), lubeluzole (Hernández-Guijo et al., 1997), and ITH33/IQM9.21 (Maroto et al., 2011). The slow I_{Ba} blockade of mibefradil reminds that of dotarizine and the extremely slow blockade exerted by NNC reminds that of R56865 and lubeluzole. An additional feature of some of these blockers as for instance lubeluzole (Hernández-Guijo et al., 1997) or R56865 (Garcez-do-Carmo et al., 1993) is their ability to cause the inactivation of VACCs currents, a property that is not shared by NNC and mibefradil in the present experiments, neither by dotarizine in previous experiments (Villarroya et al., 1995). This gradual blockade could be linked to a time dependent progressive accumulation of NNC and mibefradil at the plasmalemma of CCs, as the case is for R56865, dotarizine, and lubeluzole, as well as for another array of so-called wide-spectrum blockers of VACCs having a high octanol/water partition coefficient (Lara et al., 1997). In this context, the slow development of VACCs blockade exerted by mibefradil and particularly NNC, should be

considered when using them as pharmacological probes to block a particular $[Ca^{2+}]_c$ signal and its associated physiological or physiopathological function. In fact, their potencies to block such function could be considerably higher if the experimental design included a period of several minutes to allow the equilibration of mibefradil and NNC with the lipid environment of their target channel.

The secretory response triggered by pulses of 75 mM K^+ was nearly fully blocked by 5 μM each of NNC and mibefradil and by 50 μM Ni^{2+}. At 75 mM, K^+ drives the membrane potential of CCs from -60 to 0 mV (Orozco et al., 2006); at this highly depolarised membrane potential the L, N, and PQ high-VACCs are opened and therefore, their blockade by the high concentrations of NNC, mibefradil, and Ni^{2+} could explain the pronounced blockade of such response.

To explore the effects of NNC, mibefradil, and Ni^{2+} on the HIS response of RECCs, we first considered their ability to block I_{Ba} and hence, the high-VACCs, at threshold concentrations (IC_{20}) and at intermediate concentrations (IC_{50}) (table 1). The blockade of the HIS response exerted by 25 (2 x IC_{20} to block I_{Ba}) and 41 μM Ni^{2+} (IC_{50} to black I_{Ba}) was 44% and 60%. In the case of mibefradil the blockade exerted by 0.9 μM (IC_{20} to block I_{Ba}) was 35% and that evoked by 4.4 μM (IC_{50} to block I_{Ba}) was 71%. However, in the case of NNC, at 0.4 μM (the IC_{20} to block I_{Ba}) the blockade of the HIS response was already near maximum (73%). This indicates that the blockade elicited by mibefradil and Ni^{2+} at their IC_{50} concentrations likely involved the blockade of high-VACCs, while the blockade exerted by 0.4 μM NNC (its IC_{20}) likely involved VACCs other than the L, N, and PQ, most probably the T-type channels. This is consistent with the initial study of the effects of NNC on the various subtypes of VACCs expressed in HEK293 cells; in this heterologous system NNC blocked T channel currents with an IC_{20} of 6.8 μM, but the high-VACCs currents were not affected even at concentrations of 100 μM (Huang et al., 2004). The native high-VACCs of CCs seem to be more susceptible to blockade by NNC, with IC_{50} of 1.8 μM for BCCs and 2.1 μM for RECCs. In spite of this, the judicious use of threshold concentrations of NNC to block the high-VACCs, namely at submicromolar concentrations,

could be highly useful to further explore the contribution of T channels to the HIS response at early life, as well as other function of CCs at embryonic or neonatal life; Ni^{2+} and mibefradil seems to have more limitations to distinguish between high- and low-VACCs mediated functional responses of CCs.

Three conclusions emanate from this study: (1) NNC, mibefradil, and Ni^{2+} cause a full concentration-dependent blockade of high-VACCs of BCCs and RECCs; (2) the low-VACCs of the T-subtype expressed by CCs at early life may be efficiently blocked by threshold concentrations of NNC that do not ostensibly block the high-VACCs of RECCs; and (3) the experiments with NNC add evidence in support of the previous suggestion that T channels are controlling the HIS response in neonatal rat adrenal slices (Levitsky & López-Barneo, 2009). However, early (Thompson et al., 1997; Takeuchi et al., 2001; Adams et al., 1996) and more recent observations (Fernández-Morales et al., 2014) suggest that L channels also contribute to the regulation of the HIS response at early life. How L and T channels interact in the regulation of such response is an interesting question that requires new experimental approaches to be answered. The judicious use of low concentrations of nifedipine and NNC and the cell exposure to sufficient time to allow drug-receptor equilibrium, should gain in selectivity to target L and T channels, respectively, and thus contribute to clarify their role in the regulation of the HIS response.

CONFLICT OF INTEREST

No conflicts of interest, financial or otherwise, are declared by the author(s).

ACKNOWLEDGEMENTS

This work was supported by the following grants to AGG: (1) SAF 2010-21795 and (2) SAF 2013-44108, Ministerio de Economía y Competitividad, Spain; (3) CABICYC; UAM/Bioibérica, Spain; (4) We thank the continued support of Fundación Teófilo Hernando, Madrid, Spain.

BIBLIOGRAPHY

Adams, M.B., Simonetta, G., McMillen, I.C. 1996. The non-neurogenic catecholamine response of the fetal adrenal to hypoxia is dependent on activation of voltage sensitive Ca^{2+} channels. *Brain Res. Dev. Brain Res.* 94, 182-9.

Alonso, M.T., Barrero, M.J., Michelena, P., Carnicero, E., Cuchillo, I., García, A.G., García-Sancho, J., Montero, M., Alvarez, J. 1999. Ca^{2+}-induced Ca^{2+} release in chromaffin cells seen from inside the ER with targeted aequorin. *J. Cell Biol.* 144, 241-54.

Arranz-Tagarro, J.A., de Los Ríos, C., García, A.G., Padín, J.F. 2014. Recent patents on calcium channel blockers: emphasis on CNS diseases. *Expert. Opin. Ther. Pat.* 24, 959-77.

Bezprozvanny, I. & Tsien, R.W. 1995. Voltage-dependent blockade of diverse types of voltage-gated Ca^{2+} channels expressed in Xenopus oocytes by the Ca^{2+} channel antagonist mibefradil (Ro 40-5967). *Mol. Pharmacol.* 48, 540-9.

Bournaud, R., Hidalgo, J., Yu, H., Jaimovich, E., Shimahara, T. 2001. Low threshold T-type calcium current in rat embryonic chromaffin cells. *J. Physiol.* 537, 35-44.

Carabelli, V., Marcantoni, A., Comunanza, V., de Luca, A., Díaz, J., Borges, R., Carbone, E. 2007. Chronic hypoxia up-regulates alpha1H T-type channels and low-threshold catecholamine secretion in rat chromaffin cells. *J. Physiol.* 584, 149-65.

Carbone, E. & Lux, H.D. 1984. A low voltage-activated, fully inactivating Ca channel in vertebrate sensory neurones. *Nature* 310, 501-2.

Carbone, E., Calorio, C., Vandael, D.H. 2014. T-type channel-mediated neurotransmitter release. *Pflugers Arch.* 466, 677-87.

Catterall, W.A. 1998. Structure and function of neuronal Ca^{2+} channels and their role in neurotransmitter release. *Cell Calcium* 24, 307-23.

de Diego, A.M.G., Gandía, L., Padín, F., García, A.G. 2014. Calcium Channels for Exocytosis and Endocytosis: Pharmacological Modulation. In: L.M. Botana (ed) Seafood and Freshwater

Toxins: Pharmacology, Physiology, and Detection. Pp. 1091-1140. 3er Ed., CRC Press, Boca Raton.

Douglas, W.W., Poisner, A.M. 1961. Stimulation of uptake of calcium-45 in the adrenal gland by acetylcholine. *Nature* 192, 1299.

Fang, L.M., Osterrieder, W. 1991. Potential-dependent inhibition of cardiac Ca^{2+} inward currents by Ro 40-5967 and verapamil: relation to negative inotropy. *Eur. J. Pharmacol.* 196, 205-7.

Fernández-Morales, J.C., Cortés-Gil, L., García, A.G., de Diego, A.M. 2009. Differences in the quantal release of catecholamines in chromaffin cells of rat embryos and their mothers. *Am. J. Physiol. Cell Physiol*.297, C407-18.

Fernández-Morales, J.C., Padín, J.F., Arranz-Tagarro, J.A., Vestring, S., Garcia, G.A., de Diego, A.M. 2014. Hypoxia-elicited catecholamine release is controlled by L-type as well as N/PQ types of calcium channels in rat embryo chromaffin cells. *Am. J. Physiol. Cell Physiol.* pii: ajpcell.00101.2014. [Epub ahead of print].

Gandía, L., Borges, R., Albillos, A., García, A.G. 1995. Multiple calcium channel subtypes in isolated rat chromaffin cells. *Pflugers Arch.* 430, 55-63.

Garcez-Do-Carmo, L., Albillos, A., Artalejo, A.R., de la Fuente, M.T., López, M.G., Gandía, L., Michelena, P., García, A.G. 1993. R56865 inhibits catecholamine release from bovine chromaffin cells by blocking calcium channels. *Br. J. Pharmacol.* 110, 1149-55.

García, A.G., García-De-Diego, A.M., Gandía, L., Borges, R., García-Sancho, J. 2006. Calcium signaling and exocytosis in adrenal chromaffin cells. *Physiol. Rev.* 86, 1093-131.

Hernández-Guijo, J.M., Gandía, L., de Pascual, R., García, A.G. 1997. Differential effects of the neuroprotectant lubeluzole on bovine and mouse chromaffin cell calcium channel subtypes. *Br. J. Pharmacol.* 122, 275-85.

Hernandez-Guijo, J.M., Maneu-Flores, V.E., Ruiz-Nuno, A., Villarroya, M., Garcia, A.G., Gandia, L. 2001. Calcium-dependent inhibition of L, N, and P/Q Ca^{2+} channels in chromaffin cells: role of mitochondria. *J. Neurosci.* 21, 2553-60.

Huang, L., Keyser, B.M., Tagmose, T.M., Hansen, J.B., Taylor, J.T., Zhuang, H., Zhang, M., Ragsdale, D.S., Li, M. 2004. NNC 55-0396 [(1S,2S)-2-(2-(N-[(3-benzimidazol-2-yl)propyl]-N-methylamino)ethyl)-6-fluoro-1,2,3,4-tetrahydro-1-isopropyl-2-naphtyl cyclopropanecarboxylate dihydrochloride]: a new selective inhibitor of T-type calcium channels. *J. Pharmacol. Exp. Ther.* 309, 193-9.

Lara, B., Gandía, L., Torres, A., Olivares, R., Martínez-Sierra, R., García, A.G., López, M.G. 1997. 'Wide-spectrum Ca^{2+} channel antagonists': lipophilicity, inhibition, and recovery of secretion in chromaffin cells. *Eur. J. Pharmacol.* 325, 109-19.

Lee, J.H., Gomora, J.C., Cribbs, L.L., Perez-Reyes, E. 1999. Nickel block of three cloned T-type calcium channels: low concentrations selectively block alpha1H. *Biophys. J.* 77, 3034-42.

Levitsky, K.L., López-Barneo, J. 2009. Developmental change of T-type Ca^{2+} channel expression and its role in rat chromaffin cell responsiveness to acute hypoxia. *J. Physiol.* 587, 1917-29.

Li, M., Hansen, J.B., Huang, L., Keyser, B.M., Taylor, J.T. 2005. Towards selective antagonists of T-type calcium channels: design, characterization and potential applications of NNC 55-0396. *Cardiovasc. Drug Rev.* 23, 173-96.

Mahapatra, S., Calorio, C., Vandael, D.H., Marcantoni, A., Carabelli, V., Carbone, E. 2012. Calcium channel types contributing to chromaffin cell excitability, exocytosis and endocytosis. *Cell Calcium* 51, 321-30.

Maroto, M., de Diego, A.M., Albiñana, E., Fernandez-Morales, J.C., Caricati-Neto, A., Jurkiewicz, A., Yáñez, M., Rodriguez-Franco, M.I., Conde, S., Arce, M.P., Hernández-Guijo,

J.M., García, A.G. 2011. Multi-target novel neuroprotective compound ITH33/IQM9.21 inhibits calcium entry, calcium signals and exocytosis. *Cell Calcium* 50, 359-69.

Mishra, S.K., Hermsmeyer, K. Selective inhibition of T-type Ca^{2+} channels by Ro 40-5967. 1994. *Circ. Res.* 75, 144-8.

Montero, M., Alonso, M.T., Carnicero, E., Cuchillo-Ibáñez, I., Albillos, A., García, A.G., García-Sancho, J., Alvarez, J. 2000. Chromaffin-cell stimulation triggers fast millimolar mitochondrial Ca^{2+} transients that modulate secretion. *Nat. Cell Biol.* 2, 57-61.

Moro, M.A., López, M.G., Gandía, L., Michelena, P., García, A.G. 1990. Separation and culture of living adrenaline- and noradrenaline-containing cells from bovine adrenal medullae. *Anal. Biochem.* 185, 243-8.

Orozco, C., García-de-Diego, A.M., Arias, E., Hernández-Guijo, J.M., García, A.G., Villarroya, M., López, M.G. 2006. Depolarization preconditioning produces cytoprotection against veratridine-induced chromaffin cell death. *Eur. J. Pharmacol.* 553, 28-38.

Randall, A.D., Tsien, R.W. 1997. Contrasting biophysical and pharmacological properties of T-type and R-type calcium channels. *Neuropharmacology* 36, 879-93.

Sorensen, J.B., Nagy, G., Varoqueaux, F., Nehring, R.B., Brose, N., Wilson, M.C., Neher, E. 2003. Differential control of the releasable vesicle pools by SNAP-25 splice variants and SNAP-23. *Cell* 114, 75-86.

Takeuchi, Y., Mochizuki-Oda, N., Yamada, H., Kurokawa, K., Watanabe, Y. 2001. Nonneurogenic hypoxia sensitivity in rat adrenal slices. *Biochem. Biophys. Res. Commun.* 289, 51-6.

Thompson, R.J., Jackson, A., Nurse, C.A. 1997. Developmental loss of hypoxic chemosensitivity in rat adrenomedullary chromaffin cells. *J. Physiol.* 498, 503-10.

Todorovic, S.M. & Lingle, C.J. 1998. Pharmacological properties of T-type Ca^{2+} current in adult rat sensory neurons: effects of anticonvulsant and anesthetic agents. *J. Neurophysiol.* 79, 240-52.

Viana, F., Van den Bosch, L., Missiaen, L., Vandenberghe, W., Droogmans, G., Nilius, B., Robberecht, W. 1997. Mibefradil (Ro 40-5967) blocks multiple types of voltage-gated calcium channels in cultured rat spinalmotoneurones. *Cell Calcium* 22, 299-311.

Villarroya, M., Gandía, L., Lara, B., Albillos, A., López, M.G., García, A.G. 1995. Dotarizine versus flunarizine as calcium antagonists in chromaffin cells. *Br. J. Pharmacol.* 114, 369-76.

Villarroya, M., Olivares, R., Ruíz, A., Cano-Abad, M.F., de Pascual, R., Lomax, R.B., López, M.G., Mayorgas, I., Gandía, L., García, A.G. 1999. Voltage inactivation of Ca^{2+} entry and secretion associated with N- and P/Q-type but not L-type Ca^{2+} channels of bovine chromaffin cells. *J. Physiol.* 516, 421-32.

Wightman, R.M., Jankowski, J.A., Kennedy, R.T., Kawagoe, K.T., Schroeder, T.J., Leszczyszyn, D.J., Near, J.A., Diliberto, E.J. Jr Viveros, O.H. 1991. Temporally resolved catecholamine spikes correspond to single vesicle release from individual chromaffin cells. *Proc. Natl. Acad. Sci. U. S. A.* 88, 10754-8.

Figure captions

Fig. 1. Concentration-dependent blockade of the whole-cell Ba^{2+} current (I_{Ba}), elicited by NNC 55-0396 (NNC) in bovine chromaffin cells (BCCs, panels A, B, C) and rat embryo chromaffin cells (RECCs, panels D, E, F). I_{Ba} was recorded under the perforated-patch mode of the patch-clamp technique, using 5 mM Ba^{2+} as charge carrier, at a holding potential of -80 mV. Test pulses to various voltages had a duration of 50 ms and were given at 15 s intervals in 10 mV steps. A family of I_{Ba} traces from an example BCC was obtained upon the application of I-V protocols before (control), after 5 min of perifusion with NNC, and 5 min after its washout. Similar I_{Ba} trace families are shown in Da,b,c for an example RECC. B and E are pooled results of I-V curves for BCCs and RECCs respectively; note here the full I_{Ba} recovery with 1 μM NNC, compared with the partial recovery in A and B where 5 μM NNC was used. Concentration-response curves for the blockade of peak I_{Ba} elicited by NNC are graphed in panels C (BCCs) and F (RECCs); these data are means ± S.E.M. of the number of cells shown in parentheses from at least 3 different cultures. *P<0.05 with respect to control (Mann-Whitney´s rank-sum test).

Fig. 2. Concentration-dependent blockade of the whole-cell peak Ba^{2+} current (I_{Ba}) elicited by mibefradil and Ni^{2+} in bovine chromaffin cells (BCCs, panels A, C) and rat embryo chromaffin cells (RECCs, panels B, D). Experimental protocols are as those described in Fig. 1; peak current was elicited with test depolarising pulses to -10 or 0 mV to obtain peak current. The compounds were present 5 min before and during the test pulses. Peak currents are normalised as % of control currents in the absence of compound; a single concentration of the compounds were tested in separate cells. Data are means ± S.E.M. of the number of cells shown in parentheses from at least 3 different cultures. The IC_{50} for each compound was calculated from each graph.

Fig. 3. Time course of the blockade of the whole-cell Ba^{2+} current (I_{Ba}) elicited by NNC 55-0396 (NNC), mibefradil, and Ni^{2+} in bovine chromaffin cells (BCCs, panels A, C, E) and rat

embryo chromaffin cells (RECCs, panels B, D, F). Experimental protocol was as in Fig. 1. The compounds were applied during 3 min and the concentrations indicated by the horizontal bars in each panel. Peak current amplitudes are given in the ordinates in pA; the abscissae show the time in minutes since the braking down into the cell cytosol with the perforated-patch. Note that generally, I_{Ba} amplitudes are smaller in RECCs with respect BCCs. Data are from example cells.

Fig. 4. Concentration-dependent blockade of the K^+-evoked elevation of the cytosolic Ca^{2+} concentration, elicited by NNC 55-0396 (NNC) in bovine chromaffin cells (BCCs) and rat embryo chromaffin cells (RECCs). Cells preloaded with the Ca^{2+} probe fura-2 were challenged with a high K^+ solution (45 mM K^+ with isoosmotic reduction of NaCl and containing 2 mM Ca^{2+}) applied for 5 s at 3 min intervals (dots at the bottom of the Ca^{2+} transient traces in panels A and B). Cells were challenged with the K^+ solution before and during the application of 10 μM NNC (3 K^+ pulses, as shown by the horizontal bars on top of panels A and B, for the example BCC and RECC, respectively). Upon NNC removal, 2-3 additional K^+ pulses were applied to explore response recovery. To explore the concentration-dependent blockade of the $[Ca^{2+}]_c$ transients, a single NNC concentration per cell was tested. The concentration-dependent curves displayed in panels B (BCCs) and D (RECCs) were calculated after 1, 4, or 7 min of cell exposure to NNC. Data are normalised as % of the pre-NNC $[Ca^{2+}]_c$ transient amplitude at each of the time period of cell exposure to NNC, within each individual cell. Data in panels B and D are means ± S.E.M. of the number of cells shown in parentheses, from at least 3 different cultures.

Fig. 5. Concentration-response curves on the blockade of the K^+-elicited $[Ca^{2+}]_c$ transients, exerted by mibefradil (panel A, B) and Ni^{2+} (panels C, D) in bovine chromaffin cells (BCCs, panels A, C) and rat embryo chromaffin cells (RECCs, panels B, D). The experimental protocols and the plotting of the curves were performed as described in Fig. 4. Data are means ± S.E.M. of the number of cells shown in parentheses from at least 3 different cultures.

Fig. 6. Blockade by NNC 55-0396 (NNC), mibefrail, and Ni^{2+} of the quantal catecholamine release responses in bovine chromaffin cells (BCCs) and rat embryo chromaffin cells (RECCs) stimulated with high K^+. Three-four depolarising pulses of 30 s duration, given with a solution containing 75 mM K^+-low Na^+ and 2 mM Ca^{2+}, were sequentially applied to the example cells of panels A, B, and C (bottom horizontal bars below each trace, P1, P2, P3, P4). P1 was applied before exposure to the blocker, P2 after 30 s exposure (Ni^{2+}) or 5 min exposure (mibefradil, NNC), and P3-P4 after 5-10 min of compound washout. A, example trace of 4 amperometric spike traces produced in response to four K^+ pulses (P1, P2, P3, P4) in an example BCC; P2 was applied in the presence of NNC. B, protocol as in A but the experiment was performed in an example RECC. C to H, pooled results on the extent of the blockade of the K^+ evoked secretory response, elicited by NNC (C, F), mibefradil (D, G), and Ni^{2+} (E, H) in BCCs (C, D, E) or RECCs (F, G, H). Data are normalised as % of P1 within each cell, both as the number of secretory amperometric spikes per stimulus (right ordinates) or as the total cumulative secretion per stimulus (summatory of spike areas, left ordinates). ***P<0.001, ###P<0.001 with respect to P1 (Mann-Whitney´s rank-sum test).

Fig. 7. Blockade of the hypoxia-induced secretion (the HIS response) elicited by NNC 55-0396 (NNC), mibefradil, and Ni^{2+} in rat embryo chromaffin cells (RECCs). Cells were exposed 3 times to a hypoxic solution (below 5% O_2) for 1 min at 5 min intervals. The quantal release of catecholamine was amperometrically monitored with a carbon fibre mocroelectrode at the single-cell level. A, example secretory spike traces of the HIS responses obtained in a control RECC challenged three successive times with the hypoxic solution (P1, P2, P3). B, pooled normalised data in each cell, of total secretion per hypoxic stimulus in PC (left ordinate) or in the number of spikes per hypoxic stimulus (right ordinate). C, D, E are the normalised data obtained from experiments similar to those of panel A, but exposing the cells 5 min before and during P2 to threshold concentrations of NNC or mibefradil 5 min before and during P2; Ni^{2+} was present 30 s before and during P2. Data in panels B to E are means ± S.E.M. *P<0.05,

#P<0.05, **P<0.01, ***P<0.001, ###P<0.001 with respect to P1 (Mann- Whitney´s rank-sum test).

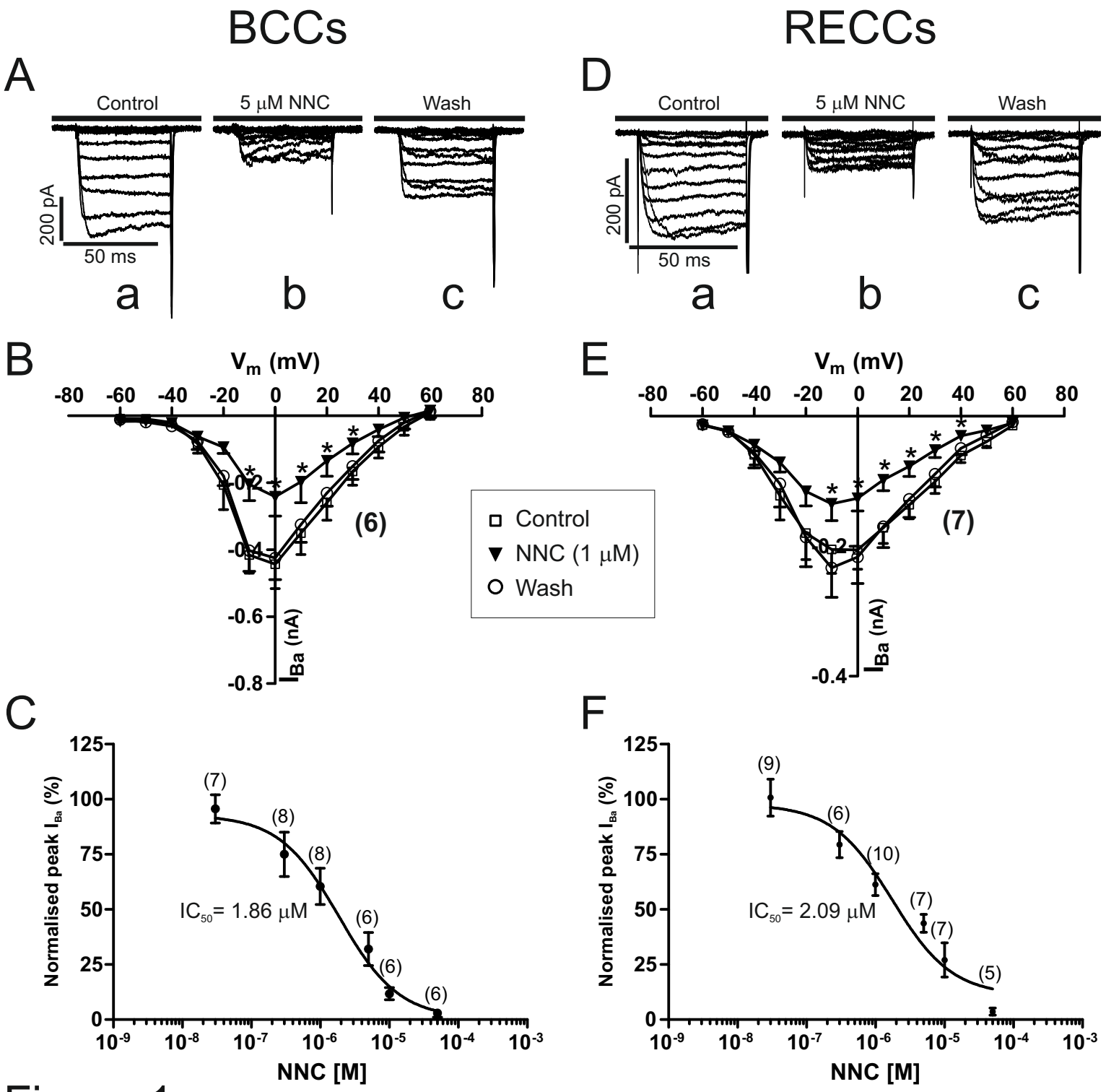
BCCs
RECCs
A
D
Control
5 μM NNC
Wash
200 pA
50 ms
a
b
c
B
E
V_m (mV)
-80 -60 -40 -20 0 20 40 60 80
-0.2
-0.4
-0.6
-0.8
I_{Ba} (nA)
(6)
(7)
Control
NNC (1 μM)
Wash
C
F
Normalised peak I_{Ba} (%)
125
100
75
50
25
0
(7)
(8)
(8)
(6)
(6)
(6)
IC_{50}= 1.86 μM
(9)
(6)
(10)
(7)
(7)
(5)
IC_{50}= 2.09 μM
10^{-9} 10^{-8} 10^{-7} 10^{-6} 10^{-5} 10^{-4} 10^{-3}
NNC [M]

Figure 1

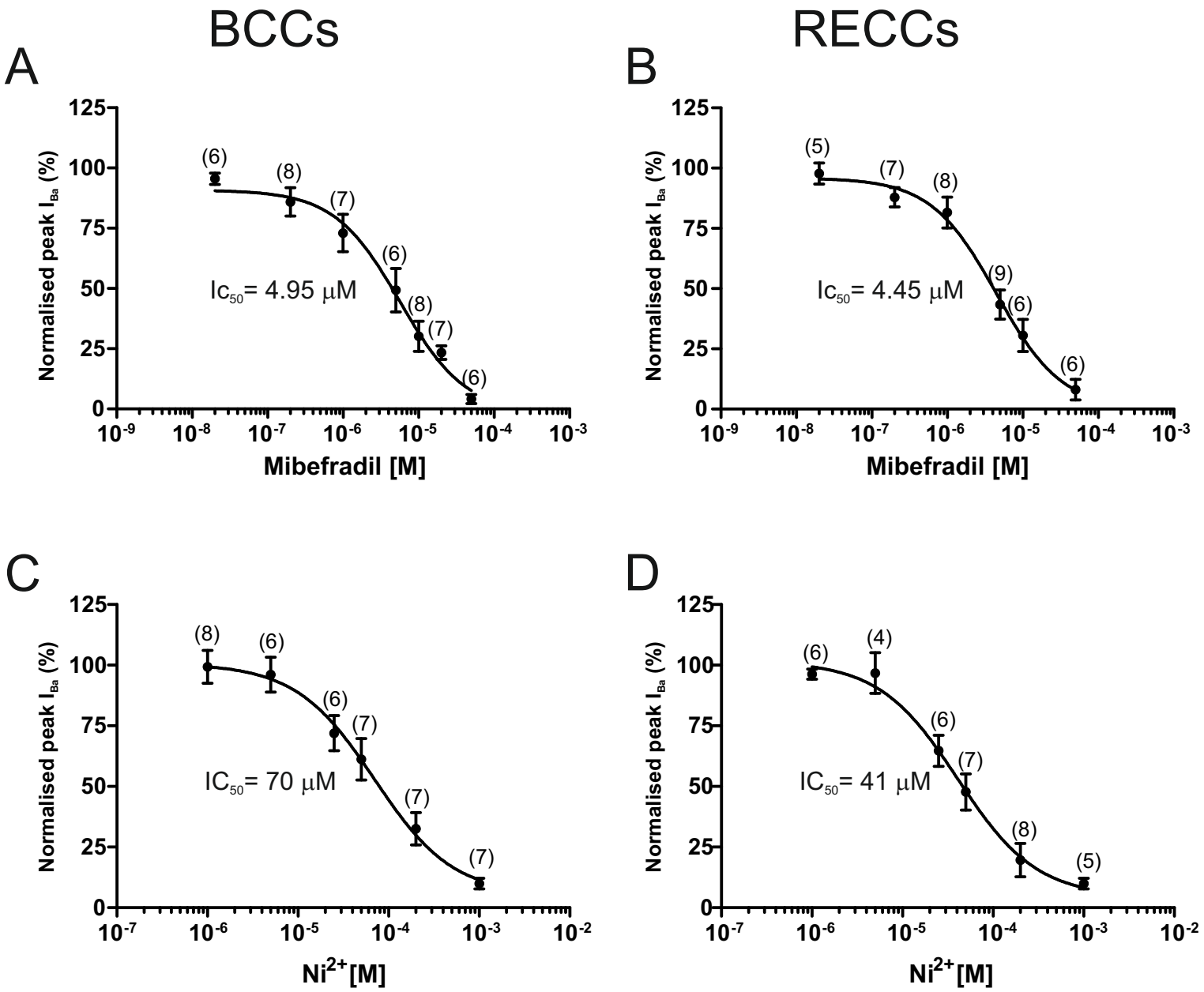
BCCs
RECCs
A
B
C
D
Normalised peak I_{Ba} (%)
Mibefradil [M]
Ni^{2+}[M]
Ic_{50}= 4.95 μM
Ic_{50}= 4.45 μM
IC_{50}= 70 μM
IC_{50}= 41 μM
(6) (8) (7) (6) (8) (7) (6)
(5) (7) (8) (9) (6) (6)
(8) (6) (6) (7) (7) (7)
(6) (4) (6) (7) (8) (5)

Figure 2

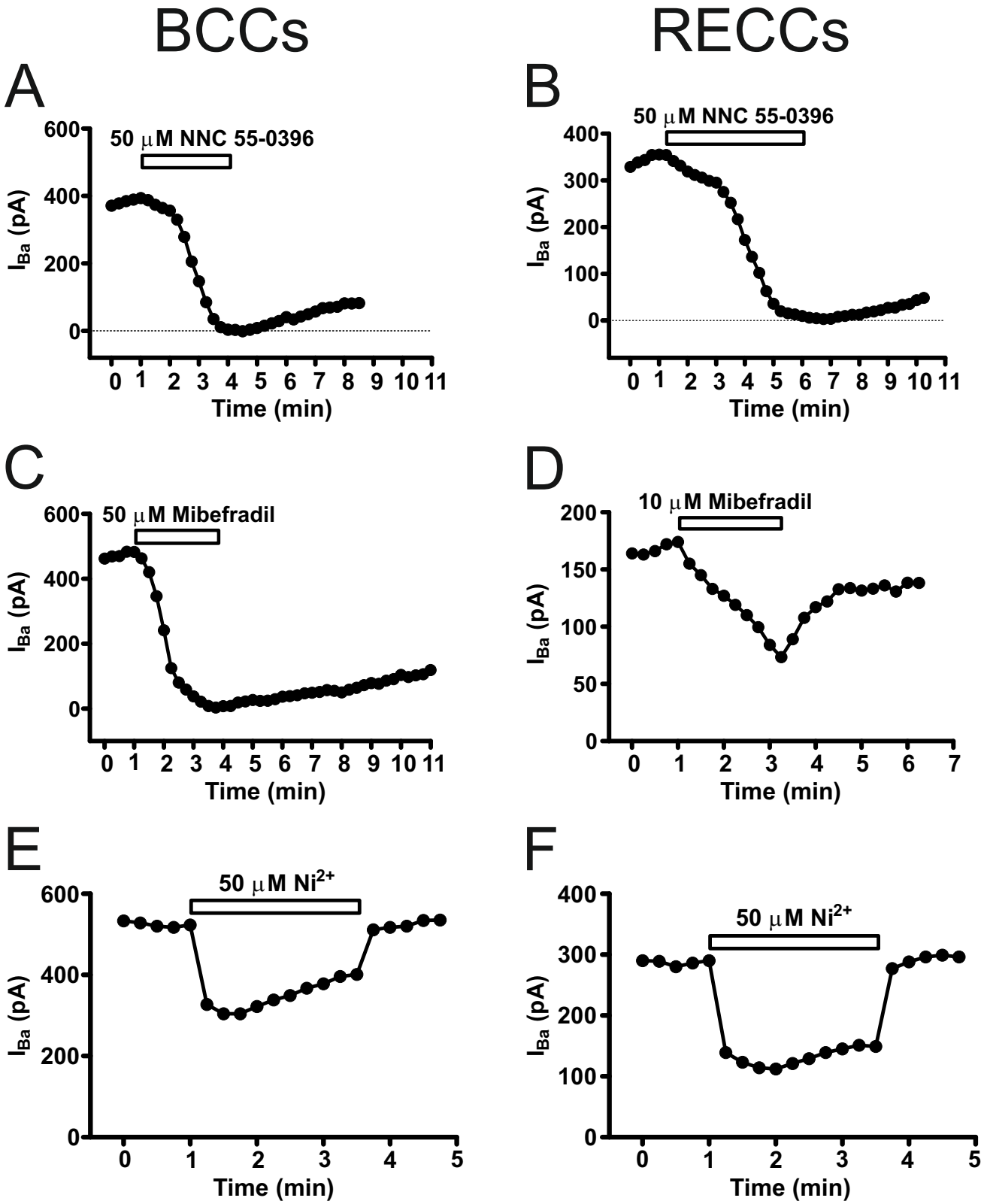
BCCs
RECCs
A
B
C
D
E
F
50 μM NNC 55-0396
50 μM NNC 55-0396
50 μM Mibefradil
10 μM Mibefradil
50 μM Ni2+
50 μM Ni2+
IBa (pA)
Time (min)

Figure 3

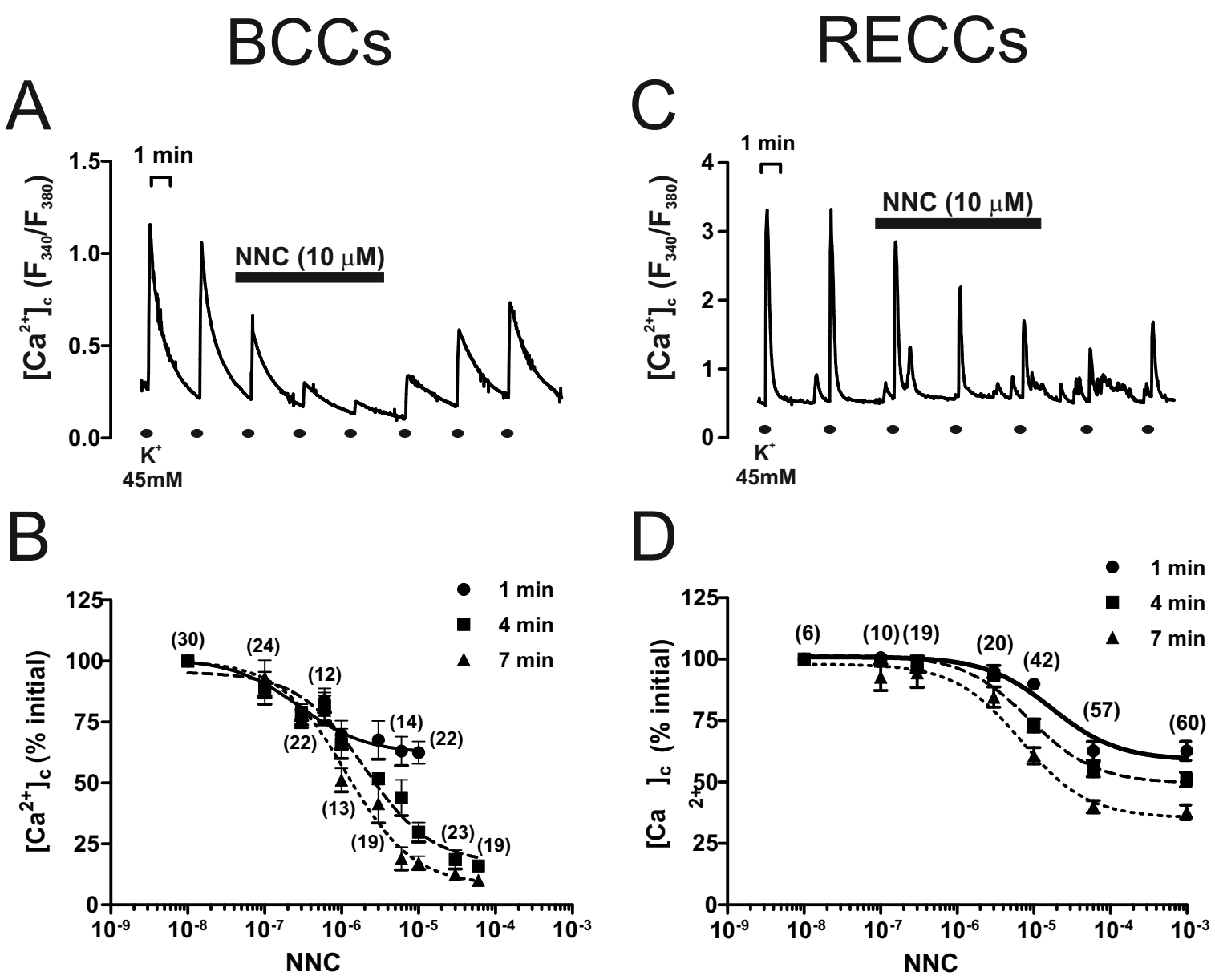
BCCs
RECCs
A
C
1 min
NNC (10 μM)
K+
45mM
[Ca2+]c (F340/F380)
B
D
1 min
4 min
7 min
[Ca2+]c (% initial)
NNC
(30)
(24)
(12)
(22)
(14)
(22)
(13)
(19)
(23)
(19)
(6)
(10)
(19)
(20)
(42)
(57)
(60)

Figure 4

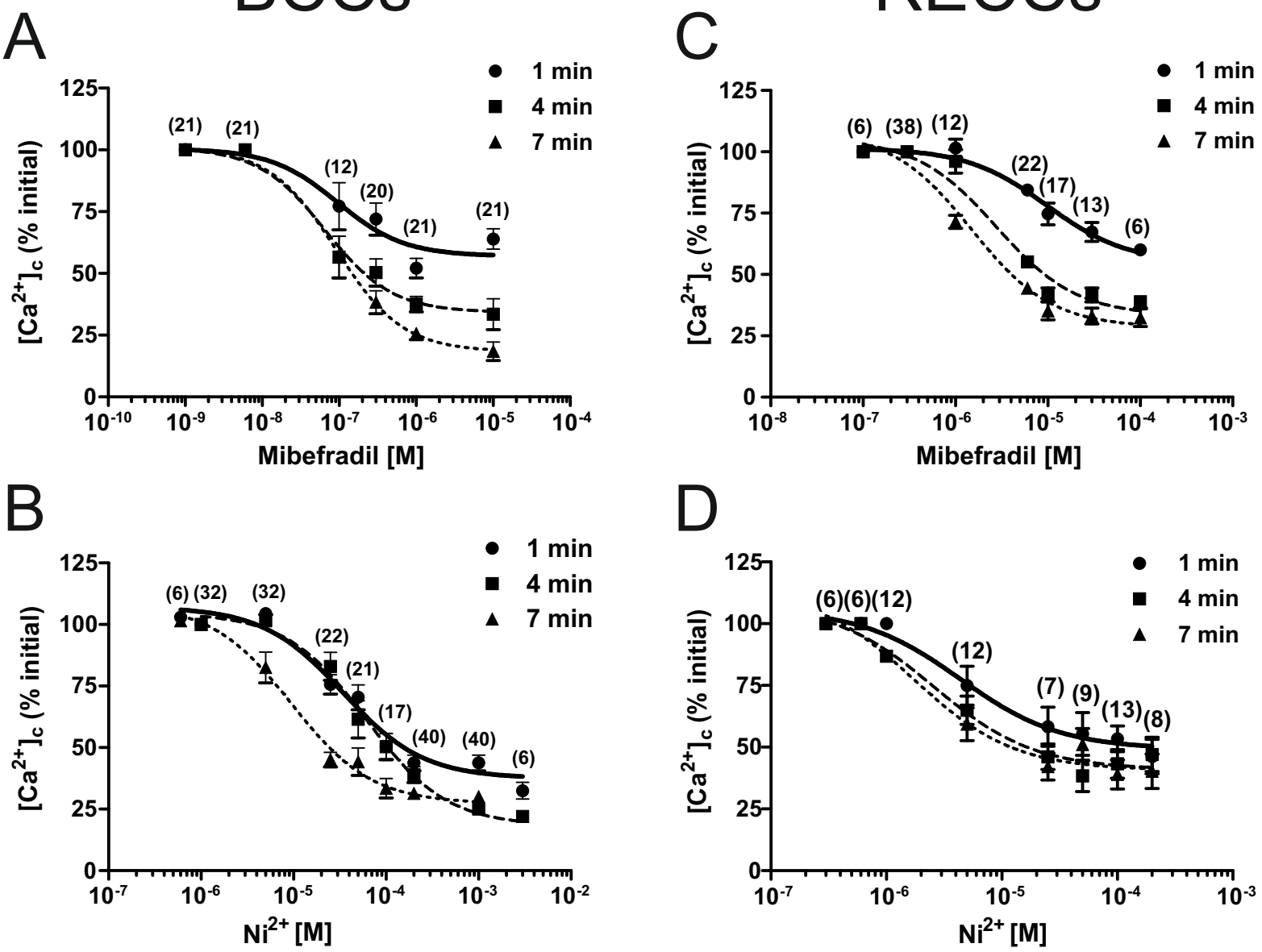
BCCs
RECCs
A
B
C
D
1 min
4 min
7 min
[Ca2+]c (% initial)
Mibefradil [M]
Ni2+ [M]
(21) (21) (12) (20) (21) (21)
(6) (32) (32) (22) (21) (17) (40) (40) (6)
(6) (38) (12) (22) (17) (13) (6)
(6)(6)(12) (12) (7) (9) (13) (8)

Figure 5

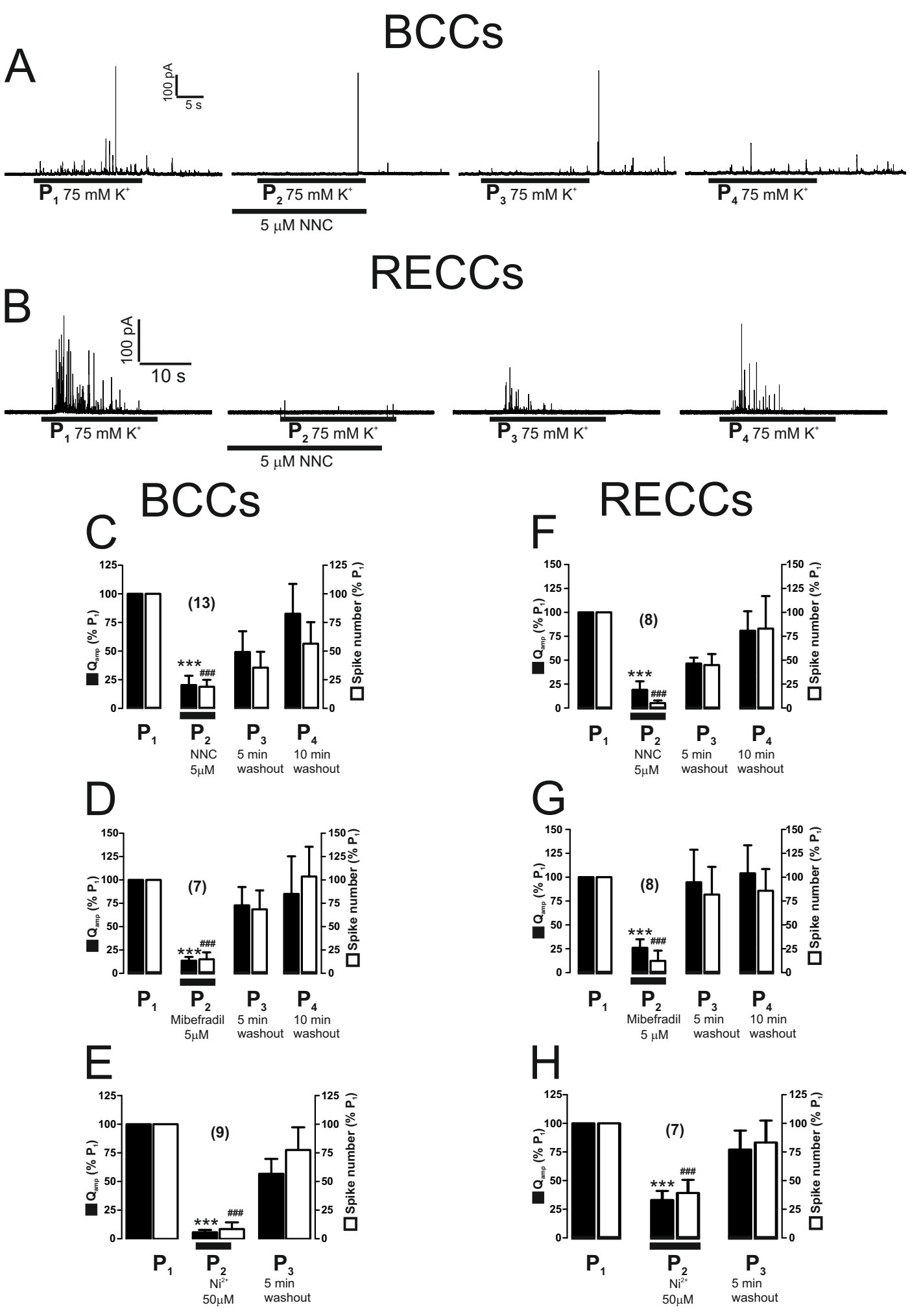
BCCs
A
100 pA
5 s
P1 75 mM K+
P2 75 mM K+
5 μM NNC
P3 75 mM K+
P4 75 mM K+
RECCs
B
100 pA
10 s
P1 75 mM K+
P2 75 mM K+
5 μM NNC
P3 75 mM K+
P4 75 mM K+
BCCs
RECCs
C
F
D
G
E
H
Qamp (% P1)
Spike number (% P1)
(13)
(8)
(7)
(9)
***
###
P1
P2
NNC 5μM
Mibefradil 5μM
Ni2+ 50μM
P3
5 min washout
P4
10 min washout

Figure 6

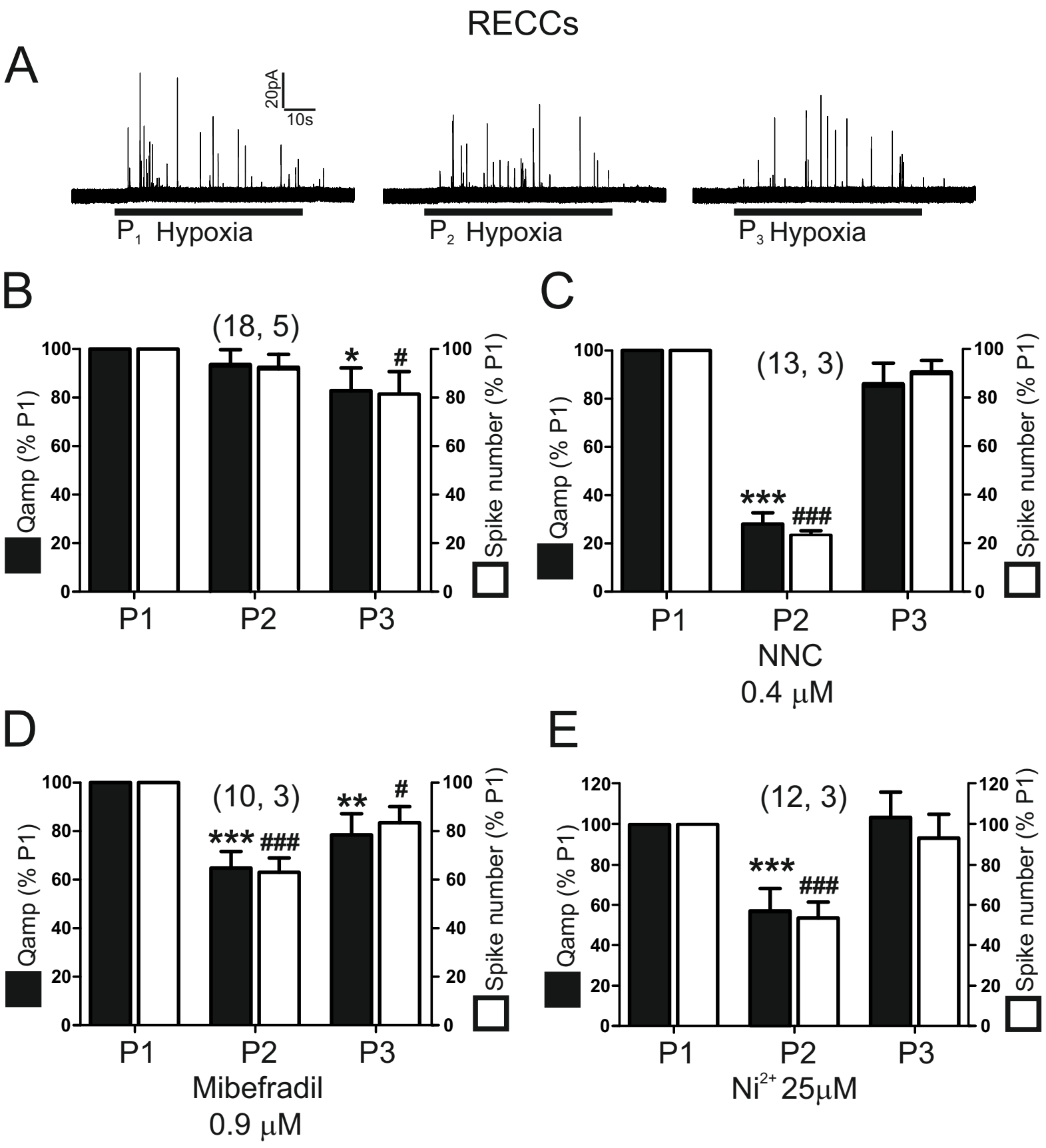
RECCs
A
20pA
10s
P1 Hypoxia
P2 Hypoxia
P3 Hypoxia
B
(18, 5)
Qamp (% P1)
Spike number (% P1)
P1
P2
P3
C
(13, 3)
NNC
0.4 μM
D
(10, 3)
Mibefradil
0.9 μM
E
(12, 3)
Ni2+ 25μM

Figure 7

Table 1. Relative blockade by Ni^{2+}, mibefradil, and NNC, of the HIS response of RECCs, exerted by a low concentration (close to the threshold concentration required to block I_{Ba} by 20%) and at an intermediate concentration (IC_{50} to block I_{Ba}). Data are means ± S.E.M. of the number of cells shown in n, from the number of different cell cultures indicated by N.

Compound	Concentration (μM)	Qamp	n/N
Ni^{2+}	25 (2 x IC_{20} I_{Ba})	44±9.5	12/3
	41 (IC_{50} I_{Ba})	60±4.9	8/3
Mibefradil	0.9 (IC_{20} I_{Ba})	35±6.7	10/3
	4.4 (IC_{50} I_{Ba})	71±4.3	7/2
NNC	0.4 (IC_{20} I_{Ba})	73±5[a]	13/3

[a] $P < 0.05$, comparing mibefradil with NNC; ANOVA-one way, with Tukey post-hoc test.

ANSWERS TO EDITOR COMMENTS Ref.: Ms. No. EJP-40809

"(…) following action is required:

- Use S.E.M. (not SE).

- To indicate statistical significance use the uppercase P instead of p."

Style changes request were done as yours suggestions.

ANSWERS TO REVIEWER COMMENTS Ref.: Ms. No. EJP-40809

REVIEWER #1

Authors of this manuscript, ***José C. Fernández-Morales, J. Fernando Padín, Stefan Vestring, Diego C. Musial, Antonio-Miguel G. de Diego and Antonio G. García,*** we would like to thank your kind positive comments to our work.

REVIEWER #2

"The study is seeking to understand the possibility of selective blockage of T-type low-voltage activated calcium channels (VACCs) in the selected cell types elucidated for embryo and neonatal life, by using several pharmacological agents for high-voltage activated calcium channels. The study's approach is a step-wise approach with patch clamp technique for measurement of several related ion channels. The results are good in quality and clearly presented. The conclusion drawn from the study is reasonable and understandable. Overall, it is a good study."

We thanks your positive comments to our study.

"Several questions for the study are as followings:

1) **It seems all the study condition (patch clamp study) for the ion channels are at room temperature at 22 °C, would it come out with a different results if running at 37 °C?"**

You are right. The path-clamp study of calcium channels currents has been performed at 22 ºC, as the myriad studies done in different laboratories. Your point on the replication of these experiments at the physiological temperature of 37 ºC is well taken. You should consider, however, that the gating and conductance of calcium channels is scarcely dependent on temperature. Additionally, we were using Ba^{2+}, instead of Ca^{2+}, as charge carrier. Unlike Ca^{2+}, Ba^{2+} does not elicit the inactivation of calcium and thus the fractional blockade by Ni^{2+}, mibefradil, and NNC 55-0396 of the whole-cell I_{Ba} should be similar at 22 ºC and 37 ºC.

2) **"Regarding the calcium channels in this study, does the mitochondrial calcium play any role into the regulations?"**

For the last 14 years, our laboratory has thoroughly investigated the contribution of Ca^{2+} buffering by mitochondria in the regulation of calcium channels, cytosolic Ca^{2+} transients, and the exocytotic release of catecholamine in chromaffin cells (see for instance our recent review García et al., Cell Calcium. 2012;51:309-20). In fact, in voltage-clamped bovine chromaffin cells, we found that the interruption with protonophores of mitochondrial Ca^{2+} buffering, caused the inactivation of calcium channels (Hernandez-Guijo et al., J Neurosci. 2001;21:2553-60). Recently, we found similar results in rat embryo chromaffin cells recording whole-cell channel

currents using Ca^{2+} as charge carrier. At present, we have this work under revision in Pflüger's Archiv; we can of course send you the graphs and/or the entire Ms. if you wish to see it.

3) **"Is hypoxia-induced secretion of catecholamine a biomarker for blockage of VACCs?"**

We have recently published a study showing that hypoxia elicited secretion from rat embryo chromaffin cells is mostly controlled by the L-subtype of voltage-activated calcium channels; the N- and PQ-subtypes channels contributed to a much lesser extent (Fernández-Morales et al., Am J Physiol Cell Physiol. 2014;307:C455-65).

4) **"In figure 7, the data is only showed for measurement of catecholamine release by low doses of the pharmacological agents, is there data show at high doses of these agents?"**

These experiments were planned to figure out if threshold concentrations of Ni^{2+}, mibefradil, and NNC 55-0396 that blocked very little the high-voltage activated calcium channels, substantially inhibited the low-voltage activated T-type channels. This was achieved only with threshold concentrations of NNC 55-0396. At higher concentrations, the HIS response will indeed be blocked by the three agents, as the case was for barium currents and K^+-elicited $[Ca^{2+}]_c$ transients.

We thank your comments that will inspire future experiments in chromaffin cells at early life.